

UNCLASSIFIED

AD NUMBER

AD840082

LIMITATION CHANGES

TO:

Approved for public release; distribution is unlimited.

FROM:

Distribution authorized to U.S. Gov't. agencies and their contractors;
Administrative/Operational Use; JUL 1968. Other requests shall be referred to Air Force Flight Dynamics Lab., Wright-Patterson AFB, OH 45433.

AUTHORITY

AFFDL ltr 1 Feb 1973

THIS PAGE IS UNCLASSIFIED

AD 840 082

AFFDL-TR-67-166

**ANALYTICAL AND EMPIRICAL INVESTIGATION
OF THE DRAG AREA OF DEPLOYMENT BAGS,
CARGO PLATFORMS AND CONTAINERS,
AND PARACHUTISTS**

E. L. HAAK

R. E. THOMPSON

University of Minnesota

TECHNICAL REPORT AFFDL-TR-67-166

JULY 1968

SEP 27 1968

This document is subject to special export controls and each transmittal to foreign governments or foreign nationals may be made only with prior approval of the Vehicle Equipment Division (FDF), Air Force Flight Dynamics Laboratory, Wright-Patterson AFB, Ohio 45433.

**AIR FORCE FLIGHT DYNAMICS LABORATORY
AIR FORCE SYSTEMS COMMAND
WRIGHT-PATTERSON AIR FORCE BASE, OHIO**

**ANALYTICAL AND EMPIRICAL INVESTIGATION
OF THE DRAG AREA OF DEPLOYMENT BAGS,
CARGO PLATFORMS AND CONTAINERS,
AND PARACHUTISTS**

E. L. HAAK

R. E. THOMPSON

This document is subject to special export controls and each transmittal to foreign governments or foreign nationals may be made only with prior approval of the Vehicle Equipment Division (FDF), Air Force Flight Dynamics Laboratory, Wright-Patterson AFB, Ohio 45433.

FOREWORD

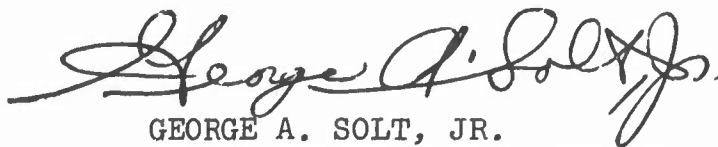
This report was prepared by the Department of Aeronautics and Engineering Mechanics of the University of Minnesota in compliance with U. S. Air Force Contract No. F 33515-67-C-1010, "Theoretical Deployable Aerodynamic Decelerator Investigations," Task 606503, "Parachute Aerodynamics and Structures," Project 6065, "Performance and Design of Deployable Aerodynamic Decelerators." The work on this report was performed between August 1, 1966, and July 31, 1967.

The work accomplished under this contract was sponsored jointly by U. S. Army Natick Laboratory, Department of the Army; Bureau of Aeronautics and Bureau of Ordnance, Department of the Navy; and Air Force Systems Command, Department of the Air Force, and was directed by a Tri-Service Steering Committee concerned with Aerodynamic Retardation. The work was administered under the direction of the Recovery and Crew Station Branch, Air Force Flight Dynamics Laboratory, Research and Technology Division. Mr. James H. DeWeese was the project engineer.

The study was conducted under the direction of Professor H. G. Heinrich in cooperation with Mr. R. A. Noreen. Several students of Aerospace Engineering of the University of Minnesota participated in the performance of the tests and data reduction. The authors wish to express their gratitude to all who rendered their services to the accomplishment of this work.

The manuscript was released by the authors in August 1967 for publication.

This technical report has been reviewed and is approved.



GEORGE A. SOLT, JR.
Chief, Recovery and Crew Station Branch
AF Flight Dynamics Laboratory

ABSTRACT

Drag areas necessary to determine the deployment characteristics of various man-carrying and cargo parachute systems are found in wind tunnel tests and surveys of existing literature. Results include the drag areas of parachute deployment bags, cargo platforms and containers, and the falling human body.

This abstract has been approved for public release and sale; its distribution is unlimited.

TABLE OF CONTENTS

	PAGE
I. Introduction	1
II. The Drag of the G-11A Cargo Platform with Various Loads	2
III. The Drag of the T-10 Parachute Deployment Bag	7
IV. The Drag of the G-11A Parachute Deployment Bag and Extraction Parachute	11
V. The Drag of the G-12D Deployment Bag and Pilot Parachute	12
VI. The Drag of the A-21 and A-22 Cargo Containers	17
VII. The Drag of the Free-Falling Human Body	21
VIII. The Drag of Uninflated Canopies	29
References	34
Bibliography	35

ILLUSTRATIONS

FIGURE		PAGE
1.	1/12 Scale Cargo Platform Model	3
2.	Wind Tunnel Arrangement of a Cargo Platform.	4
3.	Cargo Platform Model with Simulated Loads in Wind Tunnel	5
4.	Drag Coefficient versus Angle of Attack for a Cargo Platform with Containers of Various Heights	6
5.	T-10 Parachute Deployment Bag Model in Wind Tunnel	8
6.	Angle of Attack Definitions for the T-10 Parachute Deployment Bag	9
7.	Drag Coefficient of the T-10 Parachute Deployment Bag versus Angle of Attack in the Horizontal and Vertical Planes	10
8.	Configurations of the G-12D Parachute Deployment System	14
9.	Octagonal Pilot Parachute Planform	15
10.	Drag Area Ratio versus Main Canopy Line Extension for G-12D Parachute Deployment Bag and Pilot Chute in the Wake of an A-22 Cargo Container	16
11.	Drag Area versus Angle of Attack for G-12D Parachute Deployment Bag and Pilot Chute . . .	16
12.	Drag Coefficients of Simulated A-21 and A-22 Cargo Containers, $\alpha = 0^\circ$	20
13.	Drag Area of Falling Human Body as a Function of Jumper Weight and Attitude	27
14.	Drag Areas of the Human Body (from Ref 3) . .	28
15.	Test Set-Up for Uninflated Canopy Drag Area Studies	32
16.	Drag Area of an Uninflated Parachute Canopy in the Wake of an A-21 Cargo Container	33

TABLES

TABLE		PAGE
I.	Cargo Container Configurations.	19
II.	Cargo Container Drag Coefficients	19
III.	Computed Values of K for a Free-Falling Human Body.	26

SYMBOLS*

a	ratio of weights
C_D	drag coefficient
C_{D_o}	drag coefficient based on canopy surface area, S_o
$(C_D S)$	drag area
$(C_D S)_{ss}$	steady state inflated drag area
$(C_D S)_\infty$	freestream drag area
D_D	design dimension of octagonal pilot parachute
D_o	nominal canopy diameter
$D_{o_{eff}}$	effective nominal canopy diameter (reefed canopy)
d	characteristic length
h	height
K	$= (2W/C_D S)^{\frac{1}{2}}$ (Ref 4)
L_s	suspension line length
l	length
l_{si}	instantaneous suspension line length
S	area
S_o	canopy surface area
V	velocity
W	weight
w	width
α	angle of attack

Subscripts

H	heavyweight man
L	lightweight man

*As defined in Ref 1 where applicable. Additional symbols will be explained in the text where necessary.

BLANK PAGE

I. INTRODUCTION

In an earlier report (Ref 1) the characteristic forces and time relationships during deployment, inflation, and steady state were calculated for several standard parachute systems. It was found that for several systems, very little information on specific drag areas was available. This report presents the results of wind tunnel studies and literature surveys made to provide more accurate drag information and to enable a more reliable calculation of system performances. Since each system has different characteristics, the project has been divided into several essentially independent studies, each of which is a section of this report.

II. THE DRAG OF THE G-11A CARGO PLATFORM WITH VARIOUS LOADS

A. Introduction

The cargo platform used with a single G-11A parachute supports various payload shapes and sizes (Ref 1). The drag of the platform model was, therefore, measured with three different simulated loads as well as without load.

B. Models

The 1/12 scale model of a 9 ft x 8 ft cargo platform was basically a 9 in. x 8 in. plate of quarter-inch steel (Fig 1). Hollow wooden blocks, 7 in. x 7 in., with heights of 2 in. and 4 in. were utilized to simulate full-scale loads of 7 ft x 7 ft with heights of 2 ft, 4 ft, and 6 ft.

C. Test Apparatus and Experimental Procedure

The model was supported by two $\frac{1}{2}$ in. rods, and the entire assembly was mounted between the vertical force balance struts in the tunnel test section (Figs 2 and 3).

Model configurations consisted of the platform with no load and with scaled load heights of 2, 4, and 6 ft. The angle of attack was varied between 0° and 90° , where 0° angle of attack occurred when the air velocity was directed perpendicular to the base of the platform.

Drag forces were measured at air velocities of 105, 148, 181 and 209 feet per second.

D. Results

The drag coefficient, C_D , was determined by defining S to be the base area of the platform, a constant equal to 72 square inches for all configurations.

Variation of drag coefficient with angle of attack and load height is shown in Fig 4. The drag coefficient was approximately 1.25 at 0° angle of attack and was apparently independent of velocity. As one would expect, as the height of the load was increased, there was a significant increase in the drag coefficient at the higher angles of attack.

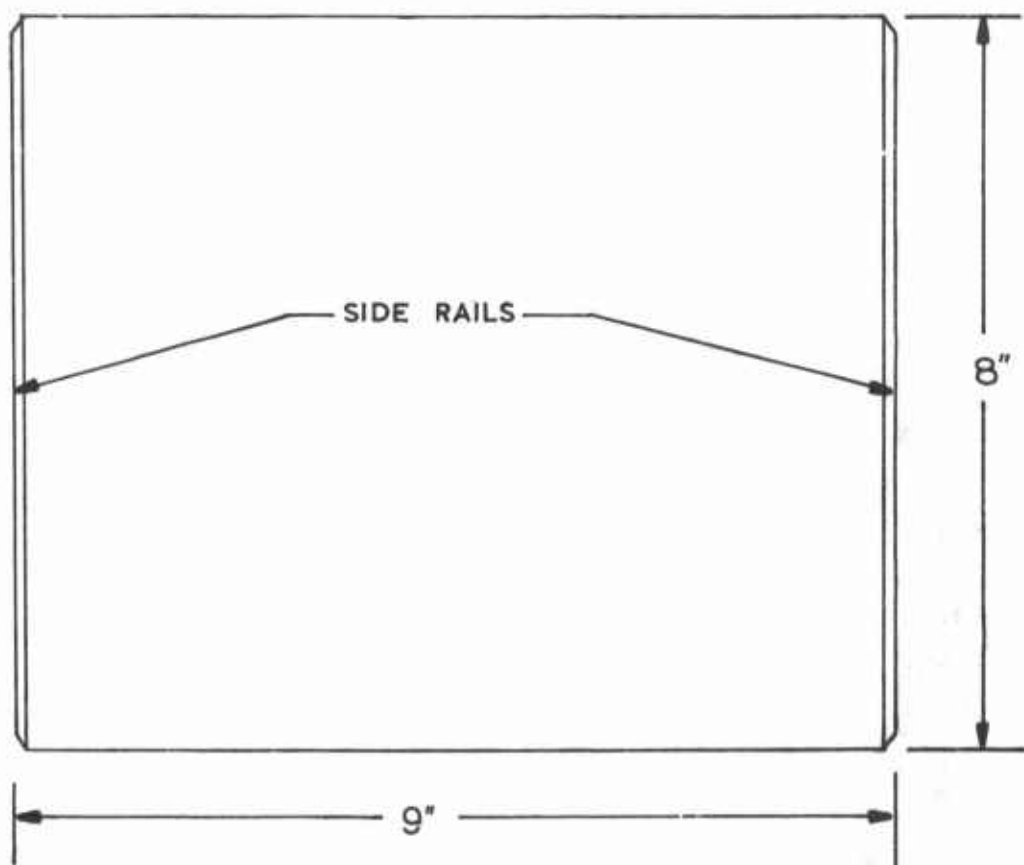
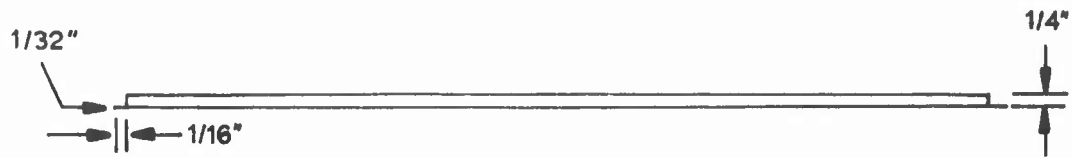
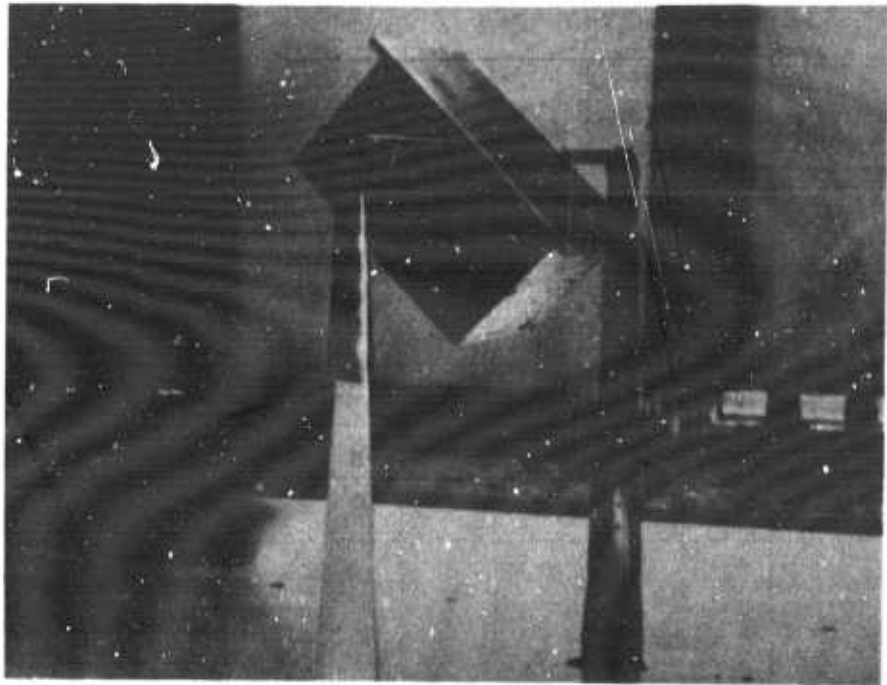


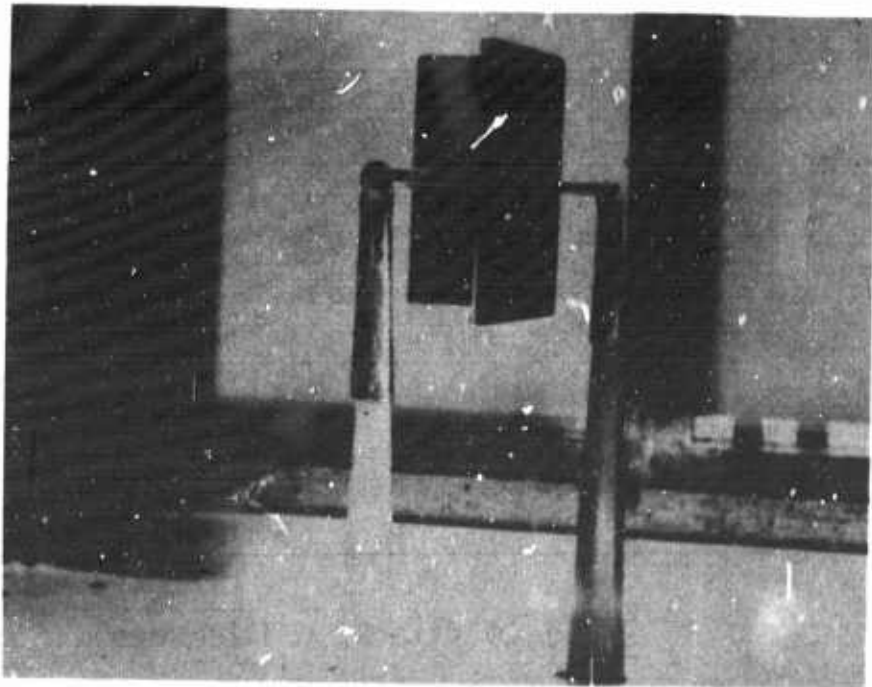
Fig 1 1/12 Scale Cargo Platform Model



Fig 2 Wind Tunnel Arrangement of a Cargo Platform



a. Model with 4" Load , $\alpha = 45^\circ$



b. Model with 2" Load , $\alpha = 0^\circ$

Fig 3 Cargo Platform Model with Simulated Loads in Wind Tunnel

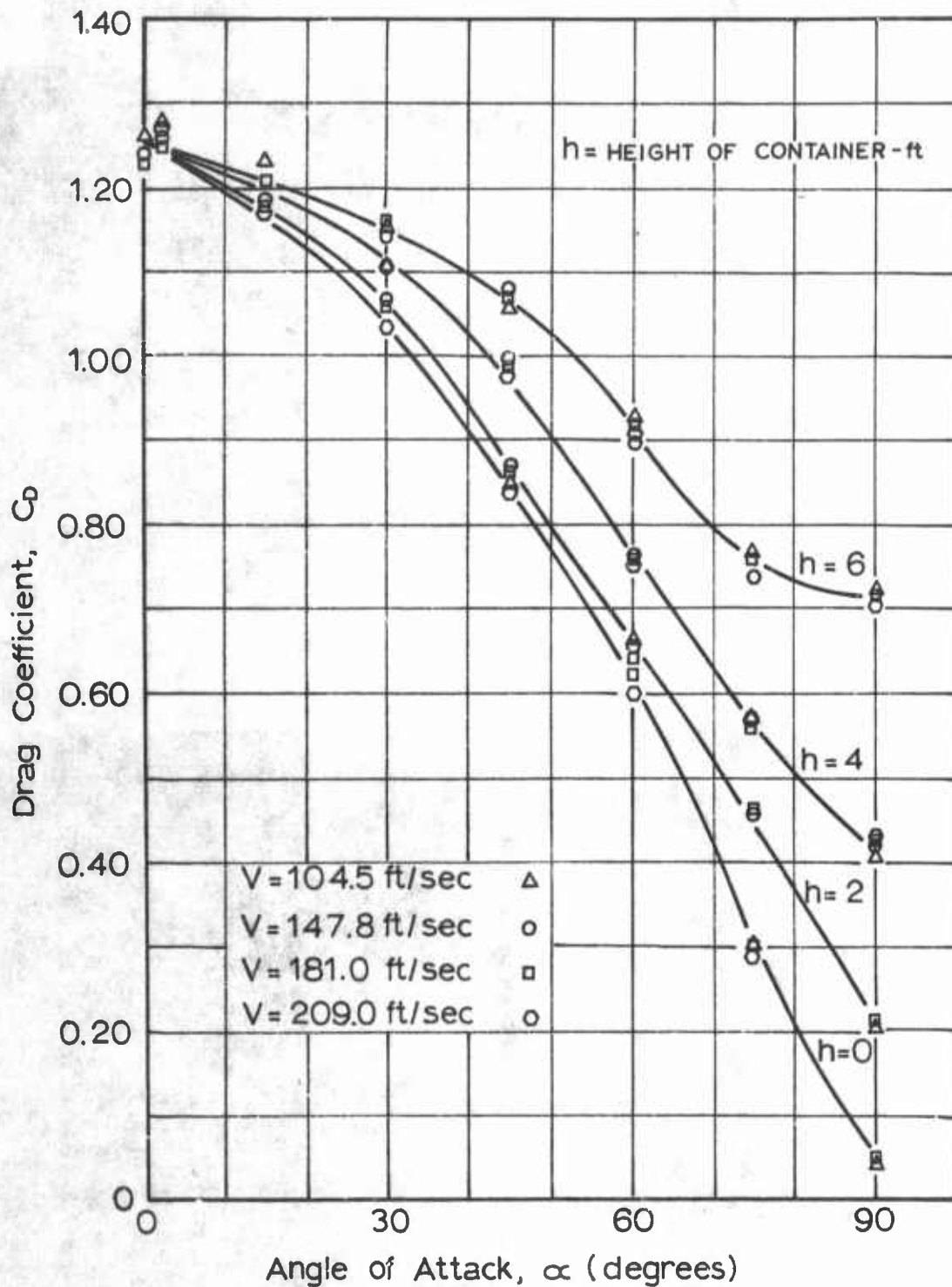


Fig 4 Drag Coefficient versus Angle of Attack for Cargo Platform with Containers of Various Heights

III. THE DRAG OF THE T-10 PARACHUTE DEPLOYMENT BAG

A. Introduction

The T-10 system is used as a static line deployed troop parachute. The drag area of the deployment bag during deployment must be known in order to calculate the deployment time, snatch velocity, and snatch force for this system (Ref 1).

B. Model

A one-half scale model of the T-10 troop parachute deployment bag was constructed having dimensions of 11 in. x 6 in. x 2.5 in. The model was made of canvas and filled by a lightweight, rectangular, wooden block.

C. Experimental Procedure

The model was tested in the same manner as the G-11A cargo platform except that an additional support was extended from the balance to the model to provide more rigidity of suspension (Fig 5).

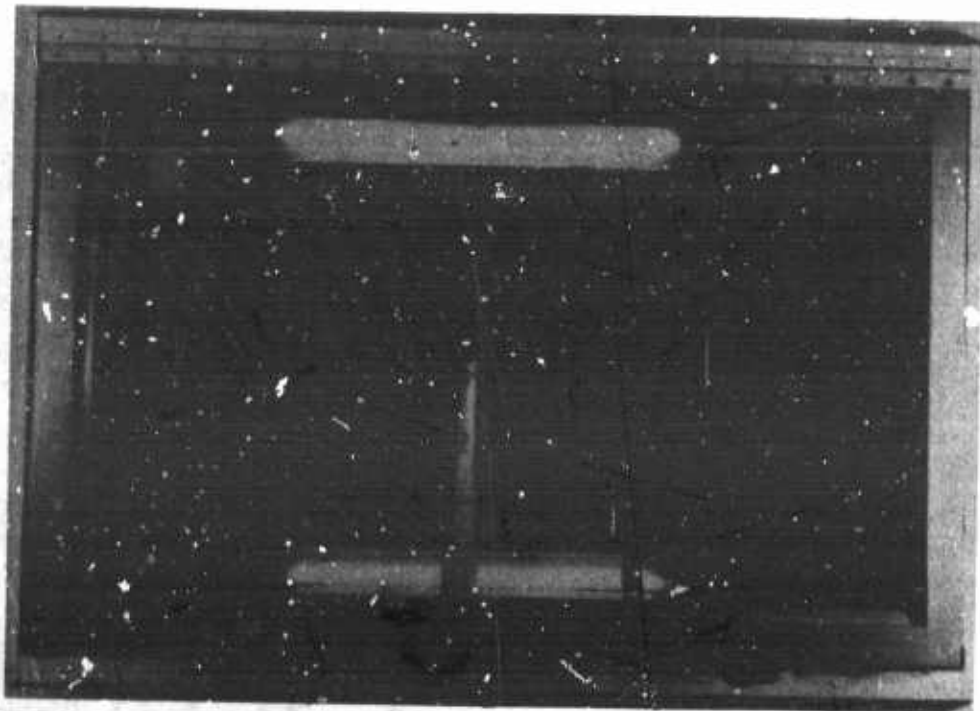
Drag forces on the deployment bag were measured at velocities of 105, 148, 181, and 209 feet per second with angles of attack ranging from 0° to 25° in both the horizontal and the vertical planes (Fig 6).

Based on the length of the bag, 11 inches, the Reynolds number of the experiments varied from 0.578×10^6 to 1.150×10^6 .

D. Results

The drag coefficient, C_D , was determined by defining S to be the area of the face with the smallest cross-sectional area, a constant equal to 15 square inches for all configurations.

Variations of drag coefficient with angle of attack in both planes are shown in Fig 7. The drag coefficient appears to be independent of velocity within the Reynolds number range and amounts to approximately 0.80 at 0° angle of attack.

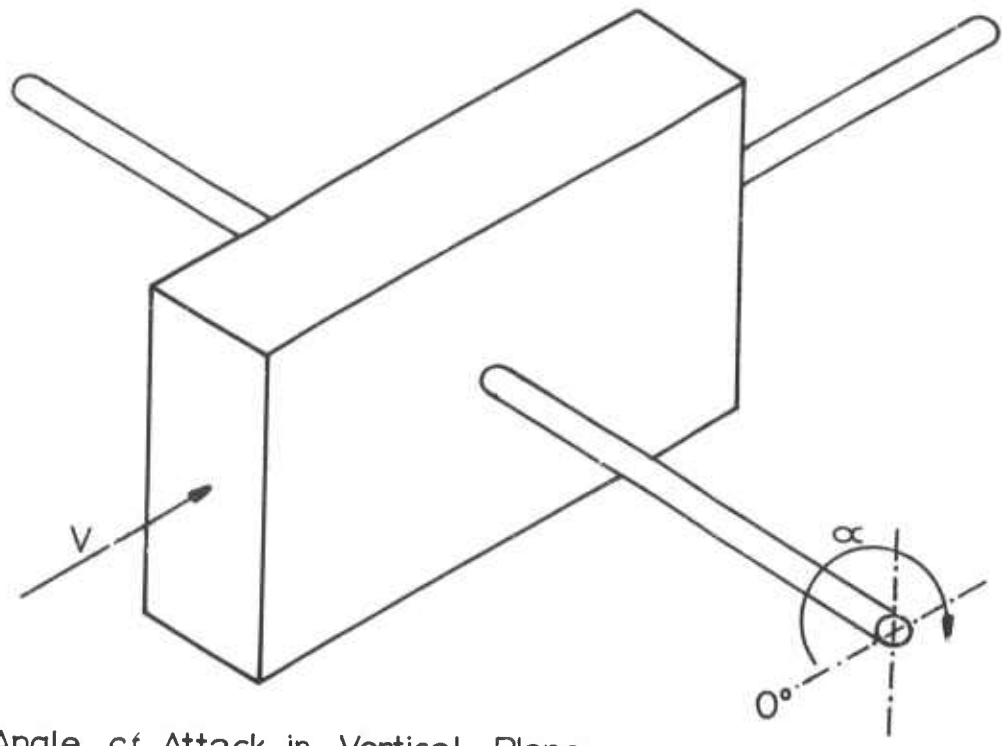


a. Angle of Attack of 25° in Vertical Plane

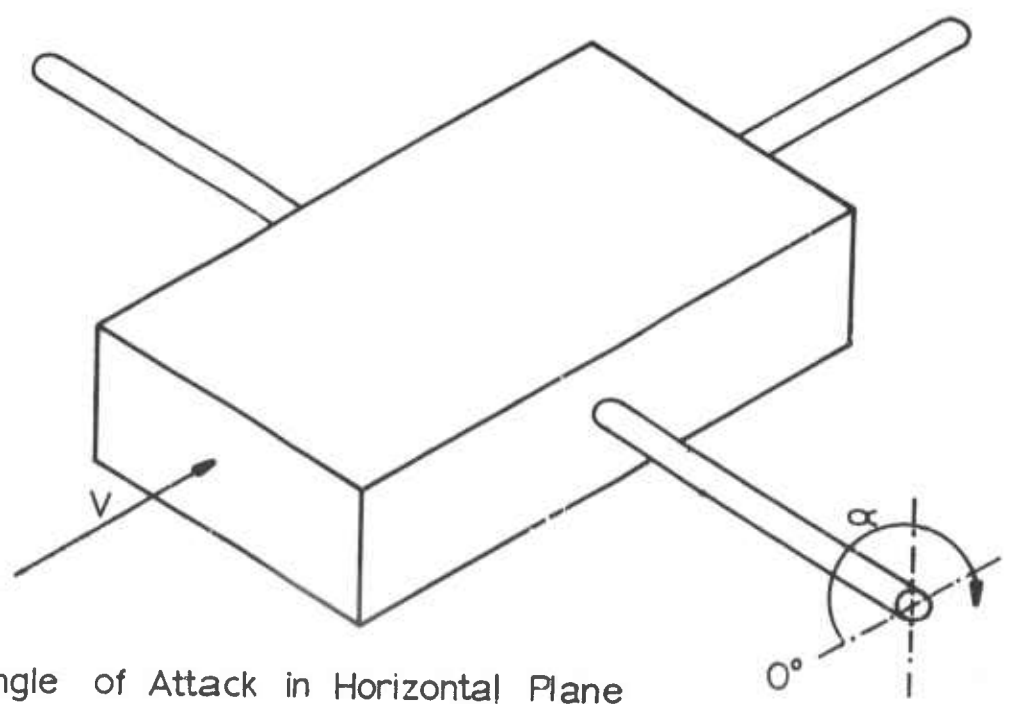


b. Angle of Attack of 0° in Horizontal Plane

Fig 5 T-10 Parachute Deployment Bag Model
in Wind Tunnel



a) Angle of Attack in Vertical Plane



b) Angle of Attack in Horizontal Plane

Fig 6 Angle of Attack Definitions for the T-10 Parachute Deployment Bag

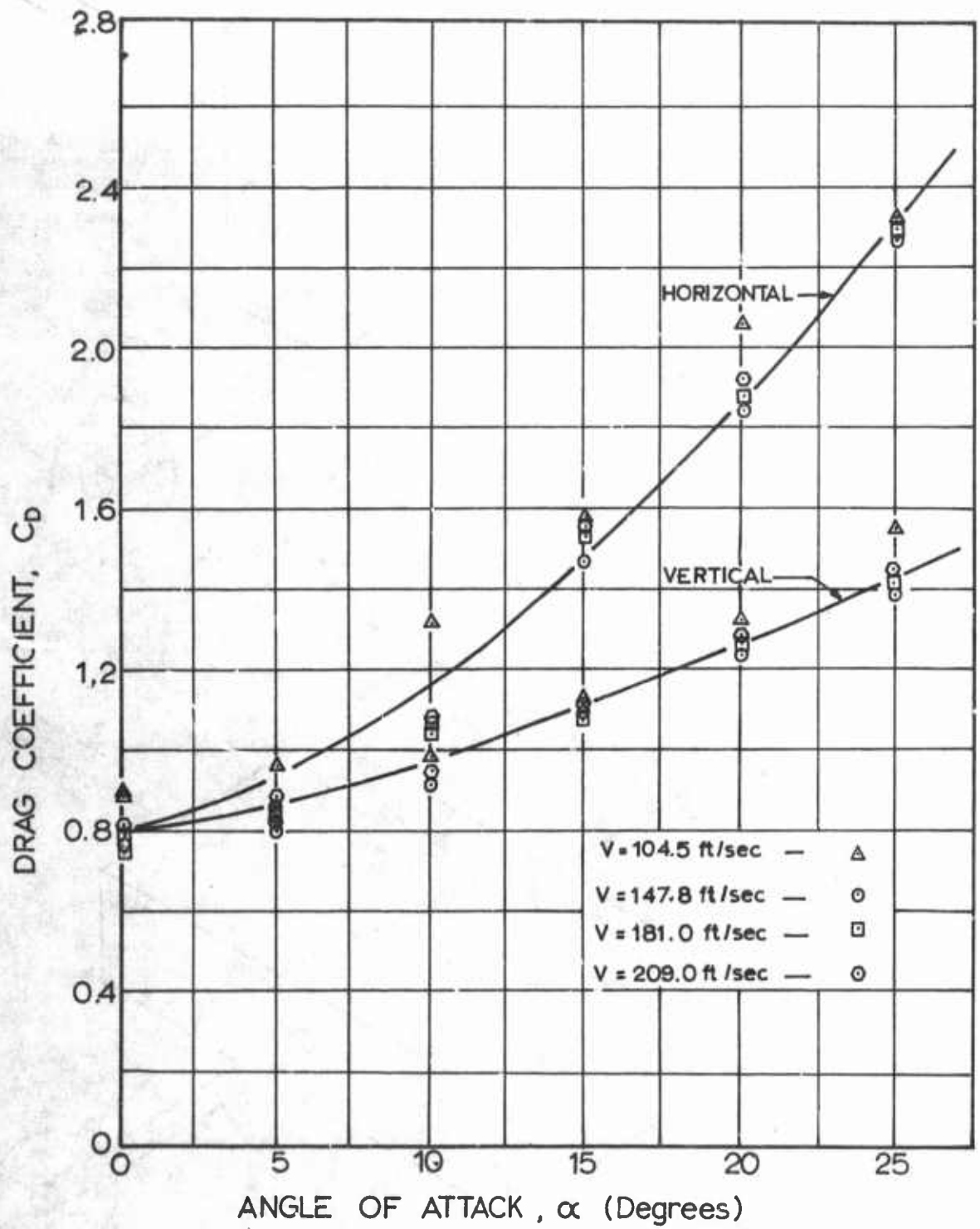


Fig 7 Drag Coefficient of the T-10 Parachute Deployment Bag versus Angle of Attack in the Horizontal and Vertical Planes

IV. THE DRAG OF THE G-11A PARACHUTE DEPLOYMENT BAG AND EXTRACTION PARACHUTE

A. Introduction

The deployment of the G-11A parachute in connection with the cargo platform described in Section II above is accomplished by means of the force of an extraction parachute; the sequence of events begins when the platform leaves the aircraft and the extraction force is transferred to the deployment bag (Ref 1).

B. Calculation of Drag Area of Deployment Bag and Extraction Parachute

For the calculation of the deployment time and the snatch force, the drag area of the deployment bag in combination with the extraction parachute has to be known.

The drag area, $C_D S$, of the 15 ft Ringslot parachute, reefed in accordance with Ref 1, is calculated by

$$(C_D S)_{\text{reefed}} = C_{D_0} \frac{\pi D_0^2}{4}$$

where D_{eff} is the effective canopy diameter. From Ref 1 the drag coefficient and the related diameter are $C_{D_0} = 0.55$ and $D_{\text{eff}} = 12$ ft, respectively. With these data, the drag area amounts to $(C_D S)_{\text{reefed}} = 62.20$ ft².

Since the G-11A deployment bag is geometrically similar to that of the T-10 parachute of the previous section, it can be assumed that the drag coefficient of the G-11A deployment bag is also 0.8. Based on the smallest cross section of the G-11A deployment bag, 12 in. x 35 in., its drag area is 2.33 ft². Therefore, the drag area of the G-11A deployment bag with extraction parachute amounts to approximately 64,5 ft².

V. THE DRAG OF THE G-12D DEPLOYMENT BAG AND PILOT PARACHUTE

A. Introduction

When the G-12D parachute is deployed by a pilot parachute, the drag area of the parachute deployment bag and its related octagonal pilot parachute must be known to calculate deployment times and forces. These values must be determined in the wake of a cargo container at various stages of deployment of the main canopy suspension lines.

B. Models and Test Configurations

This study was performed in two phases. In the first phase a 1/12 scale model of the G-12D parachute bag and pilot parachute was deployed behind a simulated A-22 cargo container (Fig 8a). The deployment bag model measured 1.25 x 2.04 x 3.33 in. and was made of plexiglas. The octagonal pilot parachute, shown in Fig 9 and described in detail in Ref 2, had suspension lines 5.50 in. long and a total canopy area of 25.20 in². The suspension lines were attached to a 9.25 in. riser. The drag of this system was measured at various locations in the wake of the simulated A-22 cargo container having the dimensions 4.33 x 3.59 x 5.00 in.

In the second phase, the drag on a 1/4 scale model of the G-12D deployment bag and its octagonal pilot parachute (Fig 8b) was measured in freestream at various angles of attack. The deployment bag was simulated by a wooden block of 3.75 x 6.125 x 10.00 in. wrapped in canvas. The octagonal pilot parachute had suspension lines 16.5 in. long and a canopy area, S, of 227 in.² (Fig 9). The suspension lines were attached to a 27.75 in. riser. The deployment bag was tested in both the vertical and horizontal planes as defined earlier in Fig 6.

As a first approximation, the results of these two test configurations may be combined to provide the required data. In the first phase, the drag reduction in the wake could be established on a small scale system, and these results could then be applied or superimposed upon the larger scale results from the variable angle of attack studies. This mode of investigation was chosen in view of the size limitation of the available wind tunnel.

C. Results

1. Effective Drag Area in the Wake

The effective drag area of the deployment bag-pilot parachute combination, (C_DS), at various stages of

suspension line deployment in the wake of the cargo container is presented in Fig 10. It can be seen that the effective drag area is already equal to the freestream drag area before 20% of the suspension lines have been deployed. This probably results from the fact that the pilot parachute, which is the primary drag producer in this system, is considerably aft of the deployment bag and quickly reaches the region where the effect of the container wake has already become very small.

2. Drag Area at Angles of Attack

Figure 11 presents the results of the tests where the deployment bag-pilot parachute combination was exposed to freestream at various angles of attack in both the horizontal and vertical planes. The drag areas indicated in Fig 11 are related to the full-scale configuration. In these tests, the angle of attack was that of the deployment bag. The pilot parachute was free to move, being restrained only by the riser line. Therefore, the variations in drag area with angle of attack shown in Fig 11 were due to the orientation of the deployment bag only.

Since the pilot parachute was statically unstable, it did not, in general, remain in the wake area but performed rather erratic motions.

D. Conclusions

From the data presented in Figs 10 and 11, it may be concluded that:

1. The drag of the pilot parachute is not significantly affected by the wake of the cargo container due to a relatively long riser and its erratic motion.

2. The drag produced by the deployment bag is almost negligible compared to the drag of the pilot parachute.

3. At a certain distance behind the container, the drag area of the deployment bag-pilot parachute combination is approximately constant at 17 ft² regardless of wake location and attitude of the deployment bag.

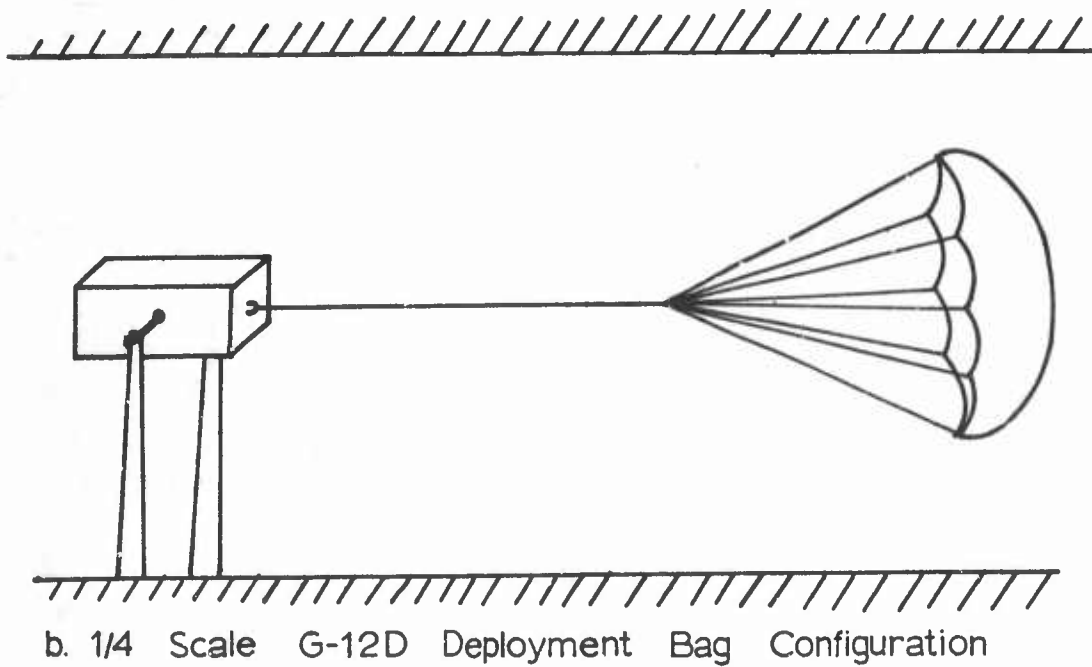
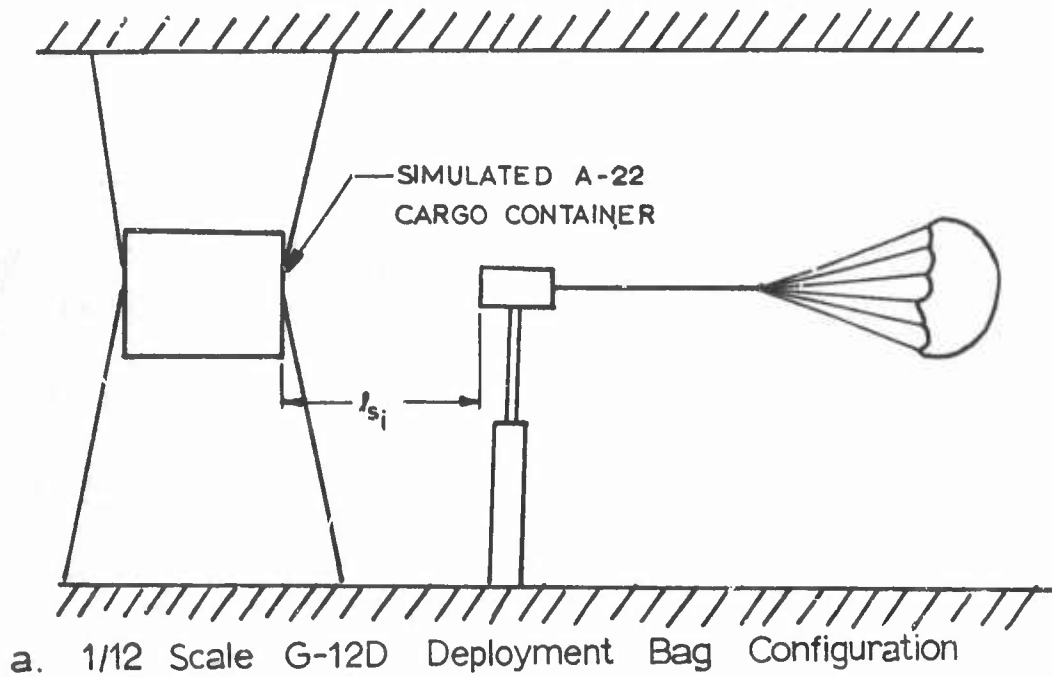


Fig 8 Configurations of the G-12D Parachute Deployment System

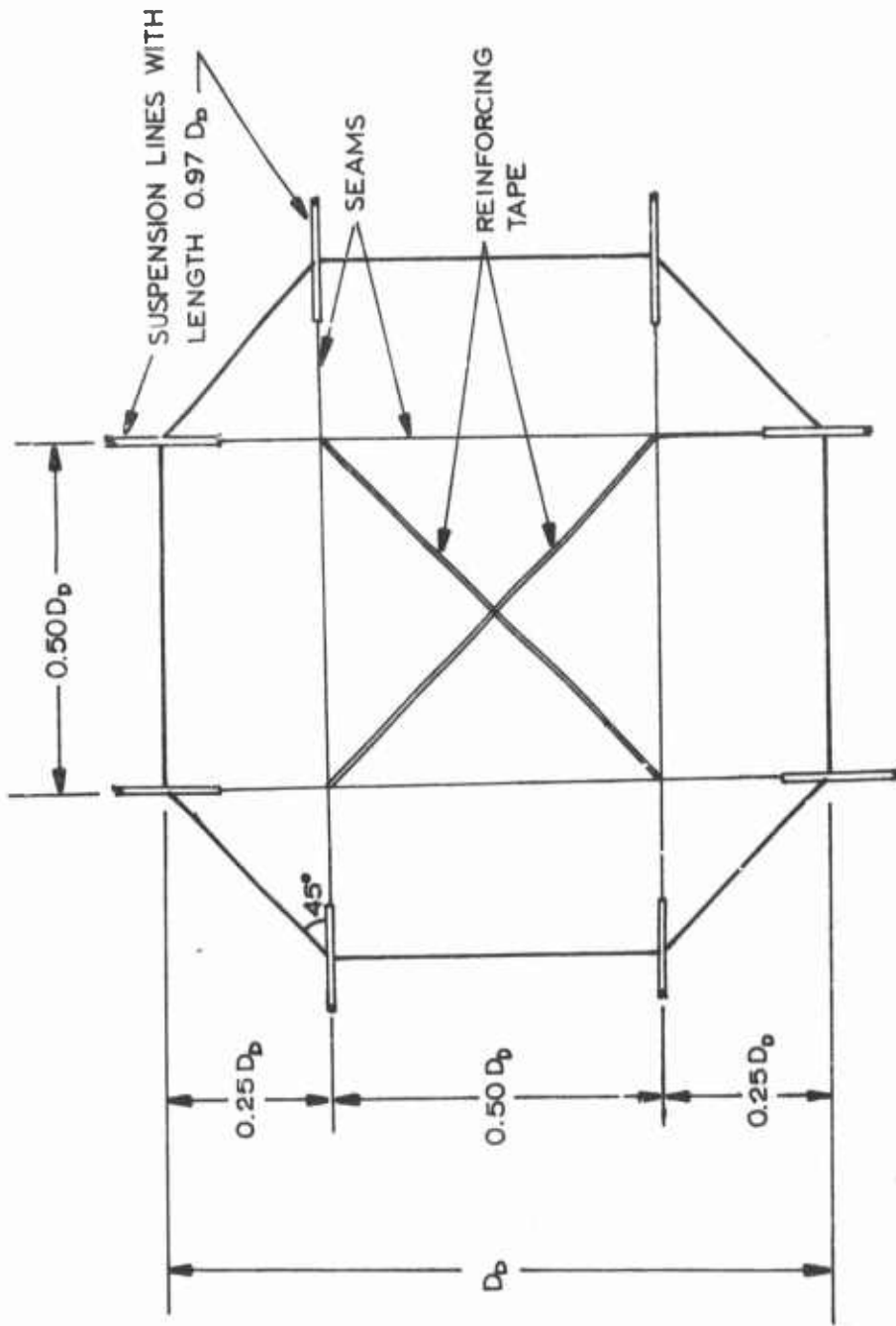


Fig 9 Octagonal Pilot Parachute Planform

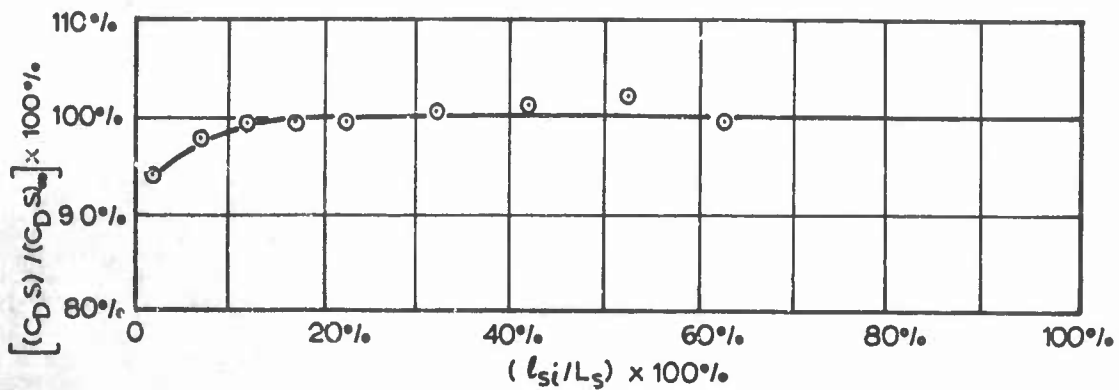


Fig 10 Drag Area Ratio versus Main Canopy Line Extension for G-12D Parachute Deployment Bag and Pilot Chute in the Wake of an A-22 Cargo Container

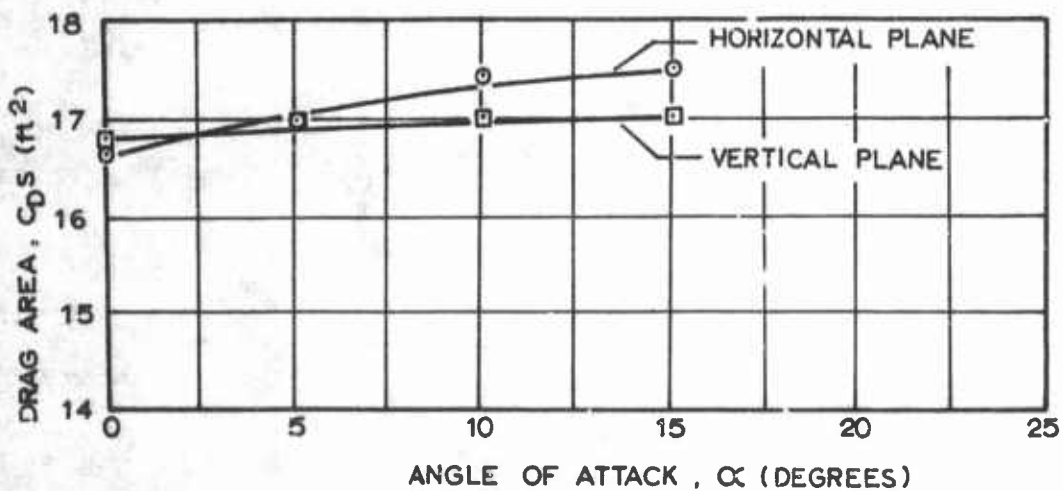


Fig 11 Drag Area versus Angle of Attack for G-12D Parachute Deployment Bag and Pilot Chute

VI. THE DRAG OF THE A-21 AND A-22 CARGO CONTAINERS

A. Introduction

The original intent of the study was to provide drag data on the A-21 and A-22 cargo containers by means of a literature survey. Unfortunately, only very limited data could be found. Therefore, cargo containers of various shapes were constructed and the drag coefficients determined through wind tunnel tests. All tests were conducted at zero angle of attack.

B. Models

The containers were rectangularly-shaped boxes made from metal and wood and wrapped in canvas. A total of ten different containers representing 19 configurations were tested (Table I). A drag coefficient for each container was determined based on the frontal area of the containers (Table II).

C. Results

The drag coefficient values of Table II, graphically presented versus the ratio h/w (Fig 12), show a distinct reduction at values of $h/w \gtrsim 1.5$. The term h/w is somewhat similar to the conventional fineness ratio. This drag change appears to be a direct consequence of the flow separation at the leading corners and the reattachment to the body surfaces downstream. Bodies with small h/w values (< 1.5) produce flow separation at the leading corners, but are too short to provide for flow reattachment. Therefore, the base pressures remain relatively low, producing a high drag force.

When the body is longer, $h/w > 1.5$, the flow reattaches to the surfaces in the $h \times l$ plane, resulting in higher base pressures and lower drag.

Similar results are shown in Ref 3 for circular cylinders in axial flow and for rectangular sections of infinite span.

It should be kept in mind, however, that the results presented in this report are for bodies with a finite length, l , and in actuality either frontal dimension, l , or w , can be used in determining the "fineness ratio". Therefore, the flow pattern descriptions with respect to the term h/w are also directly applicable for the parameter, h/l . In this study

$h/l \leq 1.00$ and it is therefore speculated in view of the above discussions that the flow over the ends of the body (i.e., the planes, $l \times w$) is always separated. With this in mind the usefulness of the presented data is limited to cases where the ratio h/l is less than about 1.5.

In the general case of a rectangular parallel-piped in subsonic flow at zero angle of attack, it appears that while opposite sides have the same flow conditions, the flow on adjacent sides can be dissimilar, depending upon the "box" dimensions.

Table I
Cargo Container Configurations

$\frac{h/l}{w/l}$	1.000	0.500	0.400	0.333	0.250	0.167
1.000	10x10x10*	10x10x5	10x10x4	---	10x10x2.5	---
0.500	10x5x10	---	10x5x4	---	10x5x2.5	15x7.5x2.5
0.400	10x4x10	10x4x5	---	15x6x5	---	---
0.333	---	---	15x5x6	---	15x5x3.75	15x5x2.5
0.250	10x2.5x10	10x2.5x5	---	15x3.75x5	---	---
0.167	---	15x2.5x7.5	---	15x2.5x5	---	---

*Figures tabulated are $l \times w \times h$ measured in inches where $l \times w$ is the frontal area of the cargo container.

Table II
Cargo Container Drag Coefficients

$\frac{h/l}{w/l}$	1.000	0.500	0.400	0.333	0.250	0.167
1.000	1.28	1.21	1.17	---	1.17	---
0.500	0.71	---	1.18	---	1.21	1.19
0.400	0.66	1.17	---	1.27	---	---
0.333	---	---	1.20	---	1.20	1.19
0.250	0.63	0.64	---	1.25	---	---
0.167	---	0.68	---	0.68	---	---

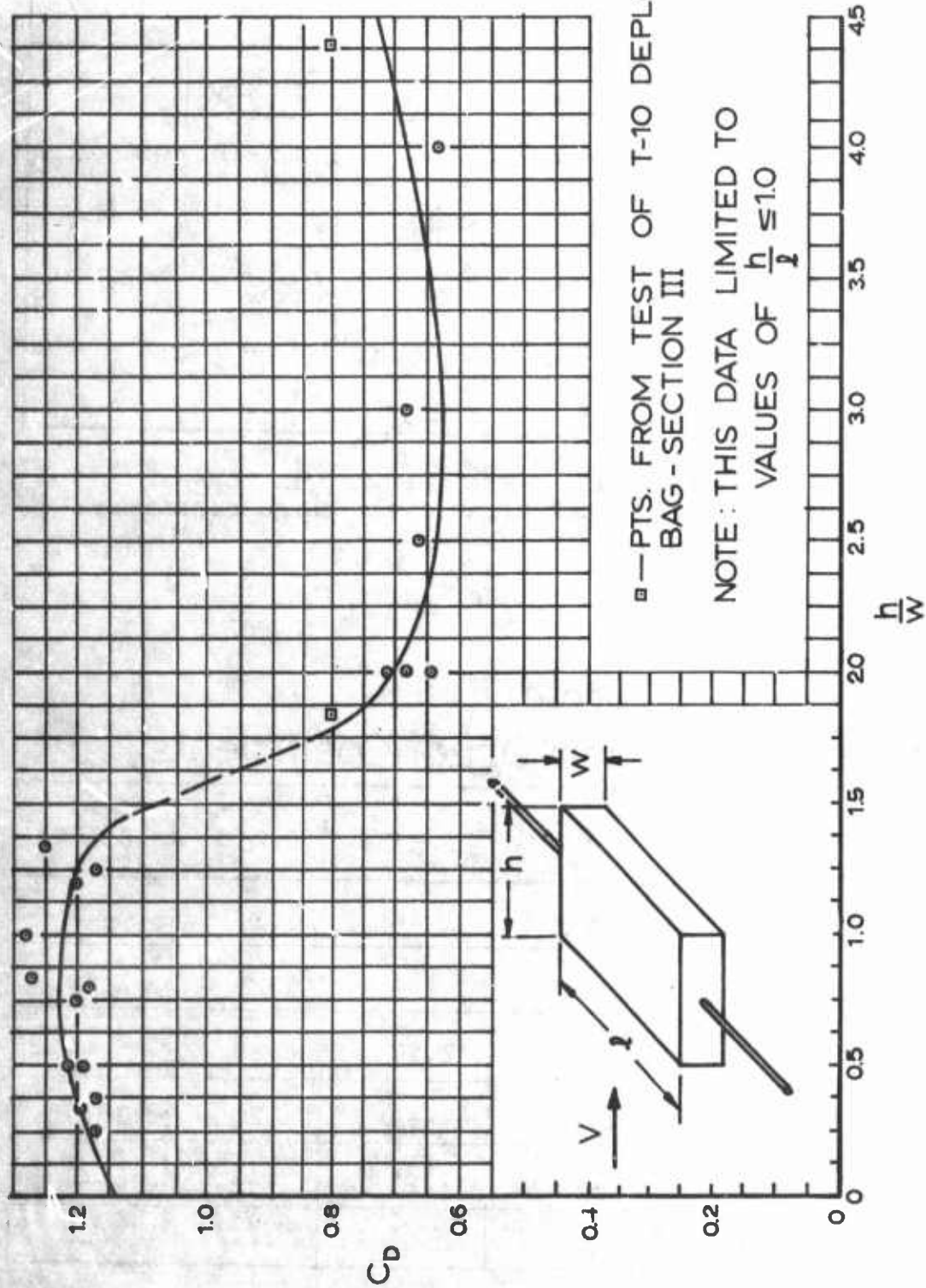


Fig 12 Drag Coefficients of Simulated A-21 and A-22 Cargo Containers, $\alpha = 0^\circ$

VII. THE DRAG OF THE FREE-FALLING HUMAN BODY

A. Introduction

In this project a literature survey was made with the intention of assembling applicable data on the drag area of the free-falling human body. The most important sources of information seem to be the publications by Webster (Ref 4), Puddycomb (Ref 5), and Hoerner (Ref 3). The contents of these publications have been studied in view of the purpose of this project, and the findings are presented below.

B. Review of Publications by Webster, Puddycomb and Hoerner

Webster has analyzed a considerable number of parachute descents and free-fall trajectories. For this study, Webster's most important contribution is the presentation of a factor K, which has some resemblance to the so-called ballistic factor frequently used in trajectory calculations.

By Webster's definition

$$K = \left(\frac{2W}{C_D S} \right)^{\frac{1}{2}}$$

in which $C_D S$ stands for the drag area and W for the weight of the man with clothing and jump equipment. The type of jump equipment is not specifically identified. The factor K is tabulated in Ref 4 and an abstract of that table is included as Table III. The values of K have been converted to drag areas and are shown in Fig 13. One notices that the drag area of the human body increases considerably with the weight of the jumper. In the light of the following dimensionless analyses, the values derived from Webster's K factor seem to be in agreement with more general considerations.

Assuming the ratio of the weight of a heavy- and a lightweight man defines a, then

$$\frac{W_H}{W_L} = a. \tag{1}$$

The weight ratio of the two human bodies must also be

$$\frac{W_H}{W_L} = \frac{d_H^3}{d_L^3} \quad (2)$$

in which d stands for a characteristic length. Equating Eqns 1 and 2, one can state that

$$\frac{d_H}{d_L} = a^{1/3} \quad (3)$$

The ratio of the surface areas of the two men may be expressed as

$$\frac{S_H}{S_L} = \frac{d_H^2}{d_L^2} \quad (4)$$

or, with Eqn 3,

$$\frac{S_H}{S_L} = a^{2/3} \quad (5)$$

One may assume that the drag coefficients of the bodies of the heavy and the light man under similar conditions of free-fall are equal. Therefore, and on the basis of Eqn 5, one may say that

$$\frac{(C_D S)_H}{(C_D S)_L} = a^{2/3} \quad (6)$$

The weight ratio of a heavy-(300 lb) and a lightweight (90 lb) man amounts to

$$\frac{W_H}{W_L} = 3.333 = a \quad (7)$$

Therefore, according to Eqn 6, the drag area ratio of these two men should amount to

$$\frac{(C_D S)_H}{(C_D S)_L} = 3.333^{2/3} = 2.231 \quad (8)$$

Now, comparing the drag area of the 90-lb man with the drag area of the 300-lb man, Fig 13 yields the ratio

$$\frac{(C_D S)_H}{(C_D S)_L} = 2.238 \quad (9)$$

This result agrees very favorably with the one obtained in Eqn 8, which indicates that the K values shown in Ref 4 and, thus, the drag area-weight relationship shown in Fig 13 of this study agrees with general principles. Further considerations in the following paragraph may be of some interest.

The equilibrium velocities (at altitude conditions) of the heavy- and the lightweight man may be expressed as

$$V_H = \left(\frac{2W}{\rho(C_D S)_N} \right)^{\frac{1}{2}} \quad (10)$$

$$V_L = \left(\frac{2W}{\rho(C_D S)_L} \right)^{\frac{1}{2}}$$

where ρ is the air density.

Combining the two velocities, one obtains

$$\frac{V_H}{V_L} = \left(\frac{W_H}{W_L} \cdot \frac{S_L}{S_H} \right)^{\frac{1}{2}}, \quad (11)$$

or with the relationships from Eqns 1 and 5, one obtains the velocity ratio

$$\frac{V_H}{V_L} = a^{1/6} \quad (12)$$

Table III in Ref 4 also gives the experimentally obtained terminal speeds (sea level conditions) for the 90- and 300-lb man, and it is shown that

$$\frac{V_H}{V_L} = \frac{151}{123} = 1.228 \quad (13)$$

On the other hand, with $a = 3.333$, Eqn 12 provides the value of

$$a^{1/6} = 1.222 \quad (14)$$

The comparison of Eqns 13 and 14 also seems to support the validity of the experimental results given by Webster.

In summary, it can be said that Fig 13 represents a good approximation of the drag area of the human body as a function of weight under the descent condition in which the jumper "rolled, somersaulted, fell head first, and so forth (Ref 4). Unfortunately, the equipment of the test jumpers has not been specified and, therefore, the absolute values of the human body drag area may have to be modified in accordance with the equipment which the jumper carries.

A newer publication by Puddycomb (Ref 5) is also concerned with instantaneous and terminal velocities of parachute jumpers between altitudes of 36,000 and 4,000 ft. In this study the descents are organized into the two weight classifications of the jumpers; namely, between jumpers of 180-200 pounds and jumpers of 150-170 pounds of body weight. The equipment which the jumper carried is specified in detail, however, in this study the total weight of the various items has not been stated. Therefore, in this study the total weight of the equipment has been estimated to be 50 lbs.

Furthermore, the descent attitudes are organized in the so-called stable prone position in which the jumper lies flat on his stomach facing the earth. The second position is the so-called stable delta attitude in which the jumper remains stretched out facing the earth, while the longitudinal axis of his body forms an angle of about 45° to the vertical. The third position is completely unstable and uncontrolled and the jumper will, in general, roll and somersault. The values for equilibrium speed given in Ref 5 for an elevation of 4,000 ft have been converted first to equilibrium speeds under sea level density conditions and then to drag areas. The information extracted in this manner is also illustrated in Fig 13.

In summary, it can also be seen that the drag areas of heavier men increase, but that their magnitude is greater than that obtained by Webster. The differences in the two sets of values may be due to different jump equipment.

In the book Fluid-Dynamic Drag (Ref 3), a schematic picture is presented illustrating the drag area, as obtained from wind tunnel tests, of the human body dressed in relatively tight-fitting clothes. Figure 14 is an abstract from Ref 3, and it is interesting to note how strongly the drag area of the human body varies with position. The application of this information, however, has to be restricted to very special cases.

C. Conclusion

From the data presented, it is apparent that the drag area of a parachute jumper may vary between $2\frac{1}{2}$ and $7\frac{1}{2}$ square feet, and the selection of the most applicable drag area value has to be made under consideration of the particular circumstances.

Table III

Computed Values of K For A Free-Falling Human Body*

Weight (lb)	Value of K (lb ^{1/2} /ft)
90	8.82
95	8.90
100	8.97
105	9.05
110	9.12
115	9.18
120	9.25
125	9.31
130	9.37
135	9.43
140	9.49
145	9.55
150	9.60
155	9.65
160	9.70
165	9.75
170	9.80
175	9.85
180	9.90
185	9.94
190	9.99
195	10.03
200	10.07
205	10.11
210	10.15
215	10.19
220	10.23
225	10.27
230	10.31
235	10.35
240	10.38
245	10.42
250	10.45
255	10.49
260	10.52
265	10.56
270	10.59
275	10.62
280	10.65
285	10.68
290	10.72
295	10.75
300	10.78

*Extracted from NACA TN No. 1315

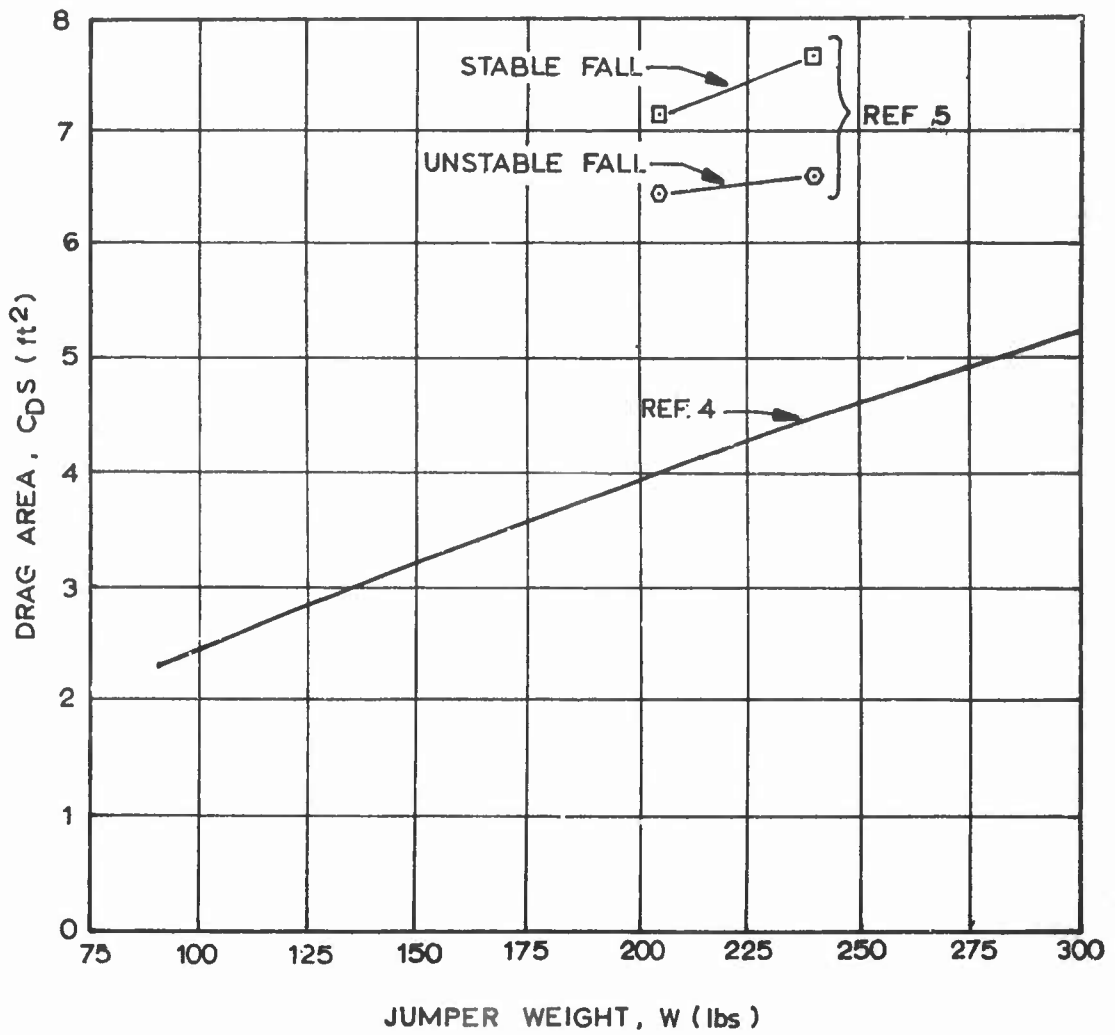
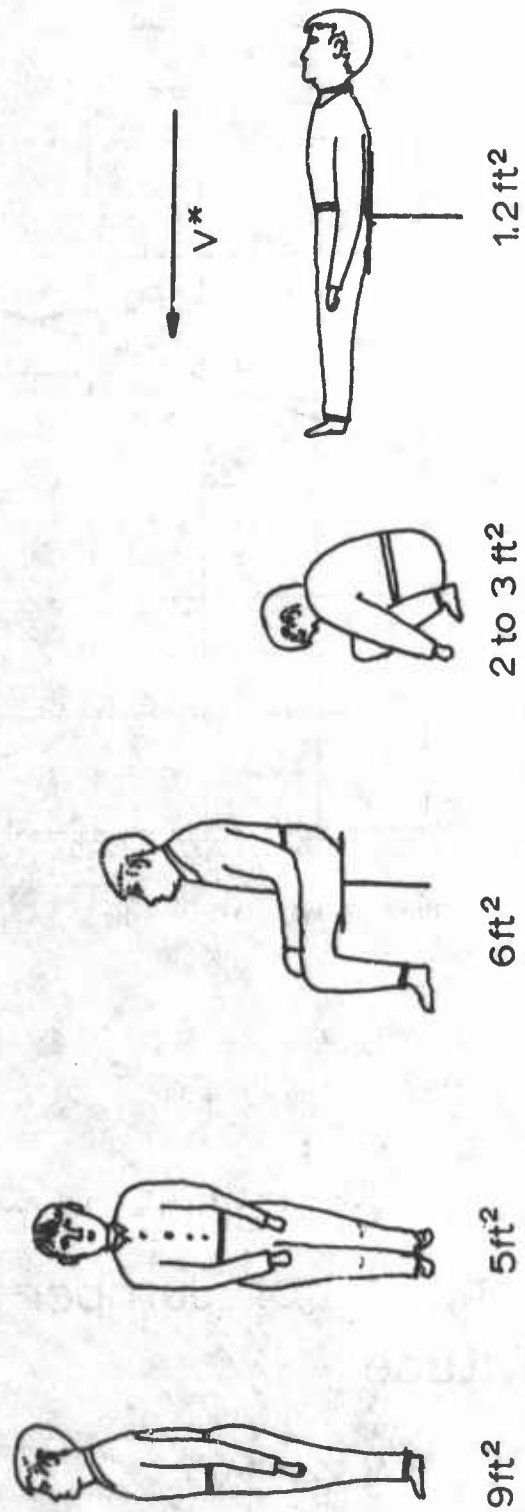


Fig 13 Drag Area of Falling Human Body as a Function of Jumper Weight and Attitude



* Relative Wind

Fig 14 Drag Areas of the Human Body (from Ref. 3)

VIII. THE DRAG OF UNINFLATED CANOPIES

A. Introduction

In a "canopy first" deployment system (Ref 1), the parachute is deployed such that the canopy is released from the pack, and it in turn deploys the suspension lines. For this case, it becomes necessary to know the drag area of the canopy as it drifts back in the airstream. This information can be applied to the T-7A and G-13 cargo parachutes as well as to the T-10 reserve parachute calculations.

B. Model

A parachute of $D_0 = 3$ ft was made for the model tests. The parachute was flat circular with 28 gores, and had a reinforced vent and skirt and heavy suspension lines to decrease the chances of damage when tested uninflated at high velocities.

The solid flat design was utilized because of the simplicity of fabrication, although it was realized that the prototype may not be a solid flat canopy. However, since the mouth of the canopy was to remain tightly closed, it was felt that the gore shape was insignificant, and the cloth surface area was the overriding parameter.

The dimensions of the full-scale A-21 cargo container were chosen to be 30 in. x 30 in. x 20 in. to coincide with the choice made in an earlier study (Ref 1).

C. Experimental Apparatus and Procedure

Drag on the canopy was recorded by transmitting the force to a cantilevered beam drag balance as shown in Fig 15. The cantilevered beam was rigidly mounted upstream of the test section. Forces were transmitted to the cantilevered beam from the uninflated parachute by a lightweight steel cable of diameter 0.030 in.

The cargo container model was mounted in the test section between two pairs of thin crosswires. The parachute model was not attached to the cargo container, but to a small loop at the downstream end of the cable, thereby measuring the drag of the uninflated parachute canopy in the wake of the cargo container without measuring the drag force on the cargo container itself. The drag force was measured at velocities of 66.2, 93.6, 114.5, 132.4, 147.6 and 162.0 ft/sec.

D. Results

The drag area of the unrestrained, uninflated canopy is presented (Fig 16) as a fraction of steady state inflated drag area, $\frac{(C_D S)}{(C_D S)_{ss}}$, at various stages of suspension line deployment.

It can be seen that the cargo container affects the drag of the canopy significantly only when the canopy skirt is in close proximity to the container. When the suspension lines are deployed to 25% of full extension, or greater, the drag area assumes a somewhat constant value.

The data show, however, some dependence upon the test velocity, with the drag area decreasing as velocity increases. In these tests the canopy was allowed to oscillate and flutter freely. High speed motion pictures at all line extensions indicated deflections of the vent section which appear to be sinusoidal with respect to time. The pictures also showed that the amplitude of vibration decreased at higher speeds while the frequency increased.

With this decreasing amplitude, it is reasonable to expect a decreasing time average of the projected area and thus a decrease in drag area at higher velocities.

The test conditions of the parachute models in the wind tunnel are comparable to those of full size parachutes which fail to inflate or are strongly reefed and moving at steady state condition. From experience it is known that streaming full size parachutes display the same general dynamic behavior as observed in the wind tunnel. However, parachutes which inflate properly do not show this whipping action during the period of deployment. This different behavior may be due to the decelerated motion and the continuously decreasing differential speed. The drag of the non-whipping canopy can be expected to be lower than that of the same canopy which flutters violently. Therefore, a new test series was conducted where the model was restrained to the wind tunnel centerline by a thin wire (Fig 15).

As expected, these additional tests yielded results in which the drag area values were approximately one-half of the freely moving values (Fig 16). In addition, the dependence of the drag area upon wind speed is significantly reduced. It is felt that these values may be more realistically applied to the deployment of unreefed full-scale systems.

The analysis above has been somewhat qualitative in nature. This is necessitated by the fact that the uninflated

parachute in a wind stream behaves in a random manner, and while general tendencies can be observed, exact measurements of some of the parameters such as frequency, amplitude and the mass distribution effects are impossible to obtain. Because of the oscillating canopies, the measured drag areas are averaged, and peak values may deviate up to + 10% from the presented curves.

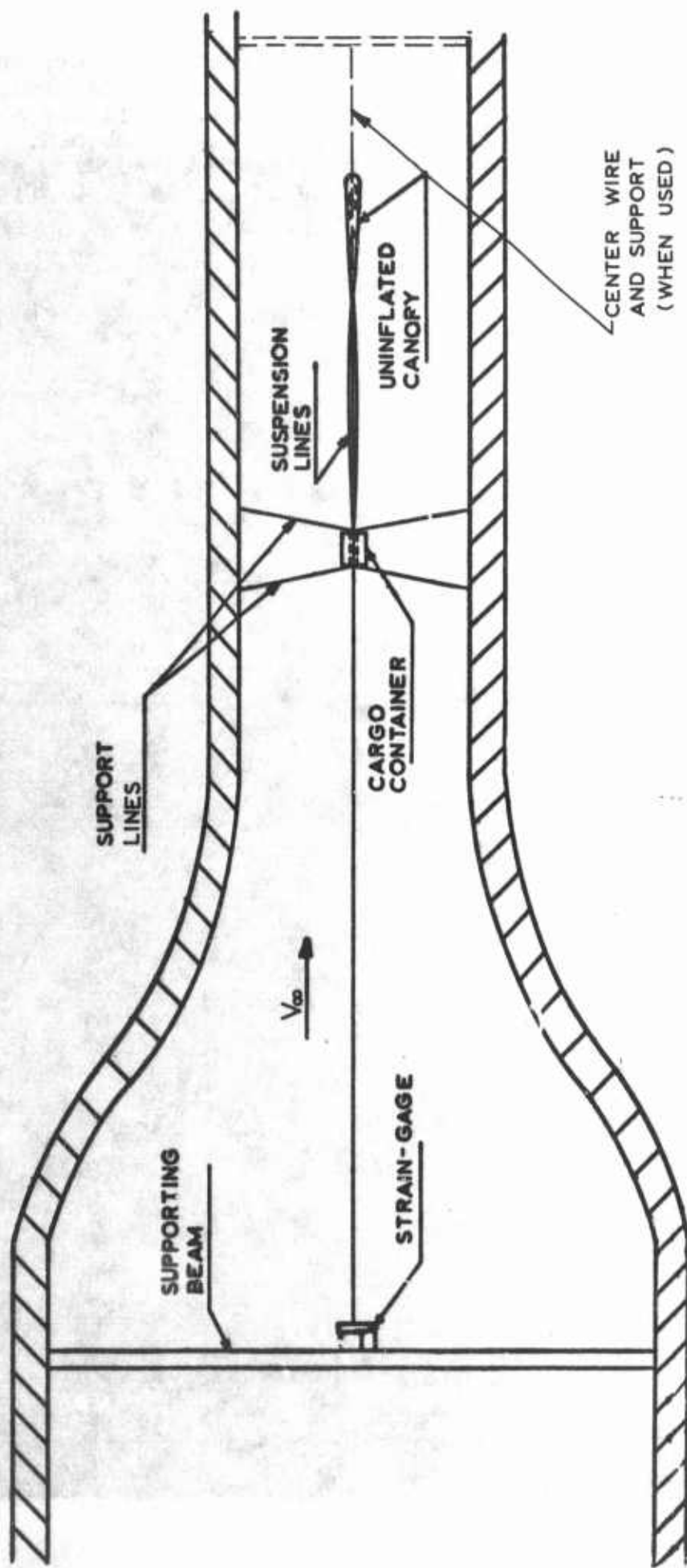


Fig 15 Test Set-Up for Uninflated Canopy Drag Area Studies

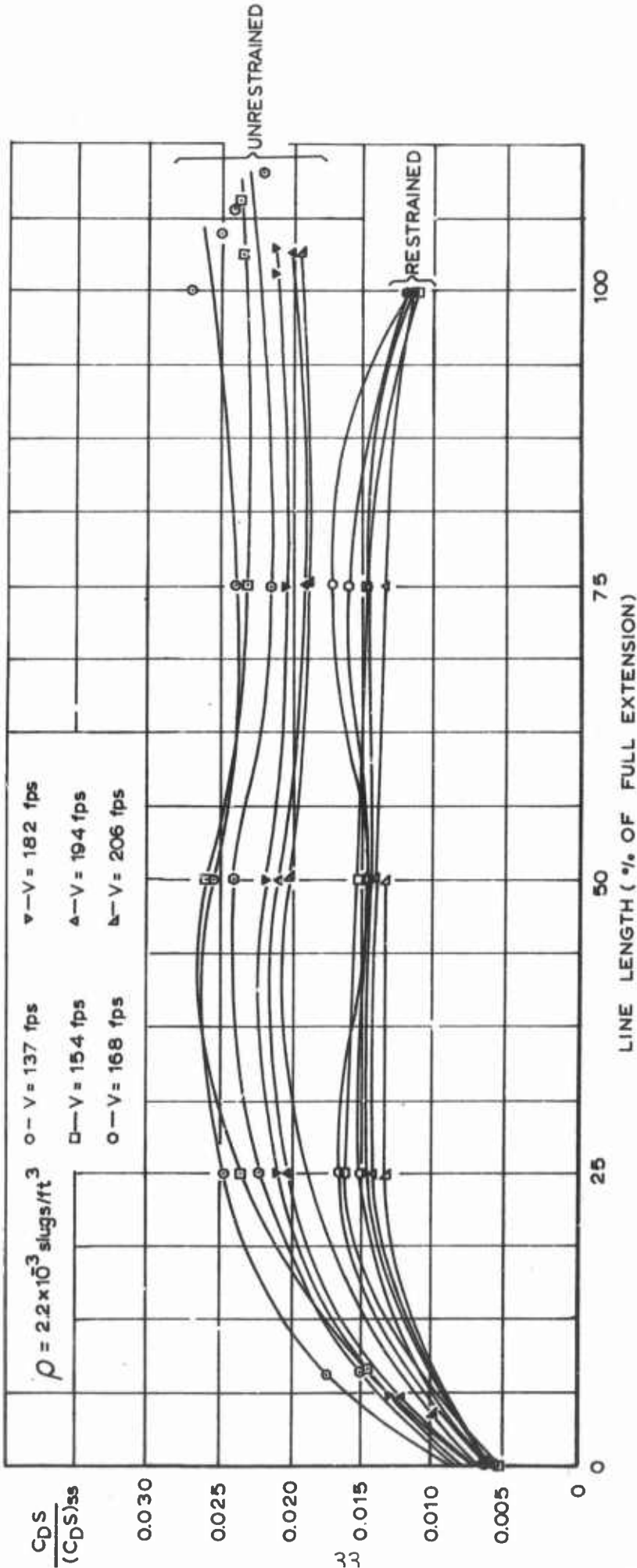


Fig 16 Drag Area of an Uninflated Parachute Canopy in the Wake of an A-21 Cargo Container

REFERENCES

1. E. L. Haak and R. V. Hovland: Calculated Values of Transient and Steady State Performance Characteristics of Man-Carrying, Cargo, and Extraction Parachutes, AFFDL-TR-66-103, July 1966.
2. United States Army Drawing No. 33E6803H.
3. S. F. Hoerner: Fluid-Dynamic Drag, Published by the Author, 1958.
4. A. P. Webster: Free Falls and Parachute Descents in the Standard Atmosphere, NACA Technical Note 1315, 1947.
5. R. H. Puddycomb: Human Free-Fall Trajectories, FTC-TDR-64-10, June 1964.

BIBLIOGRAPHY

Section VI

Heinrich, Helmut G. and Shukry K. Ibrahim: Determination of the Minimum Sized Parachute Required for Stabilization of the A-22 Cargo Container, ASD-TR-61-326, July 1961.

Ibrahim, Shukry K.: Aerodynamic Characteristics of the Parachute Stabilized A-21 Cargo Container, FDL-TDR-64-154, April 1965.

Wieselsberger, C. und A. Betz: Ergebnisse der Aerodynamischen Versuchsanstalt zu Goettingen, II. Lieferung, Verlag von R. Oldenbourg, Muenchen und Berlin, 1923.

Section VIII

Lovelace, W. R. and S. C. Allen: Parachute Descent from a Pressure Altitude of 39,750 Feet (Density Altitude, 40,200 Ft), AAF, Material Command, Eng. Div., Memo. Rep., July 9, 1943.

Maison, G. L., K. E. Penrod, and F. G. Hall: Descent Times of 200 Pound Dummies with 28-Foot Silk, 28-Foot Nylon, and 24-Foot Nylon Parachutes, AAF, Headquarters, Air Tech. Serv. Command, Eng. Div., Memo, Rep., May 30, 1945.

Unclassified

Security Classification

DOCUMENT CONTROL DATA - R & D

(Security classification of title, body of abstract and indexing annotation must be entered when the overall report is classified)

1. ORIGINATING ACTIVITY (Corporate author) University of Minnesota Minneapolis, Minnesota 55455		2a. REPORT SECURITY CLASSIFICATION Unclassified	
		2b. GROUP N/A	
3. REPORT TITLE Analytical and Empirical Investigation of the Drag Area of Deployment Bags, Cargo Platforms and Containers, and Parachutists.			
4. DESCRIPTIVE NOTES (Type of report and inclusive dates) Final Report August 1966 - August 1967			
5. AUTHOR(S) (First name, middle initial, last name) Eugene L. Haak R. E. Thompson			
6. REPORT DATE July 1968		7a. TOTAL NO. OF PAGES 36	7b. NO. OF REFS 5
8a. CONTRACT OR GRANT NO. F33615-67-C-1010		9a. ORIGINATOR'S REPORT NUMBER(S)	
b. PROJECT NO. 6065			
c. Task No. 606503		9b. OTHER REPORT NO(S) (Any other numbers that may be assigned this report) AFFDL-TR-67-166	
d.			
10. DISTRIBUTION STATEMENT This document is subject to special export controls and each transmittal to foreign governments or foreign nationals may be made only with prior approval of the Vehicle Equipment Division (FDF), AF Flight Dynamics Laboratory, Wright-Patterson AFB, Ohio.			
11. SUPPLEMENTARY NOTES		12. SPONSORING MILITARY ACTIVITY AFFDL (FDFR) Wright-Patterson AFB, Ohio	
13. ABSTRACT <p>↘ Drag areas necessary to determine the deployment characteristics of various man-carrying and cargo parachute systems are found in wind tunnel tests and surveys of existing literature. Results include the drag areas of parachute deployment bags, cargo platforms and containers, and the falling human body. () ←</p> <p>This abstract has been approved for public release and sale; its distribution is unlimited.</p>			

Unclassified

Security Classification

14. KEY WORDS	LINK A		LINK B		LINK C	
	ROLE	WT	ROLE	WT	ROLE	WT
Wind Tunnel Tests Subsonic Man-Carrying Parachute Cargo Parachutes Deployment Bag Drag Area Cargo Platform Drag Area Cargo Container Drag Area Parachutist Drag Area						

Unclassified

Security Classification